Third International Conference on CFD in the Minerals and Process Industries
CSIRO, Melbourne, Australia
10-12 December 2003

CFD SIMULATION OF SOLID-LIQUID TWO-PHASE FLOW IN BAFFLED STIRRED VESSELS WITH RUSHTON IMPELLERS

Feng WANG, Weijing WANG, Yuefa WANG and Zai-Sha MAO

Institute of Process Engineering, Chinese Academy of Sciences,
Beijing 100080, China

ABSTRACT

Three-dimensional flow field and solid concentration distribution in solid-liquid baffled stirred vessels are numerically simulated using an improved inner-outer iterative procedure. A two-fluid approach and the single phase $k-\varepsilon$ turbulence model are employed. The recirculation loop below the impeller and above the bottom is predicted. Agreement of simulation results with experimental data is satisfactory for both mean velocities of phases and solid concentration in two cases with the average solid concentration up to 20%.

NOMENCLATURE

a	coefficient of algebraic equation
b	source term in algebraic equation
c	clearance of the centreline of impeller to the bottom of the stirred vessel
C_1, C_2	constant in dissipation equation
C_b	constant in the equation of G_e
C_μ	constant in k , ε equations
d	diameter of particle
D	diameter of impeller
G	turbulence generation term
G_e	turbulence related to drag force
f	diffusive term in continuity equation
F	momentum exchange between two phases
H	height of liquid in stirred tank
k	turbulent kinetic energy
p	pressure
p'	pressure correction
r	radial coordinate
R	radius of stirred tank
R_f	Richardson number
t	time
T	diameter of stirred tank
u	velocity component
$\mathbf{u}$	velocity
w	width of blade
z	axial coordinate
σ_ε, σ_k	constants in k , ε equations
α	phase fraction
ε	dissipation
ϕ	general variable
$\boldsymbol{\omega}$	angular speed
ρ	density
μ	viscosity
ν	kinematic viscosity
i, j	i, j direction
k	k phase
eff	effective
r, θ, z	radial, azimuthal and axial
t	turbulence
tip	impeller tip

INTRODUCTION

Among the various industrial unit operations involved with multi-phase systems, agitation of solid-liquid systems is quite commonly encountered such as catalytic reactions, leaching, polymerization, etc. Despite their widespread use, the complex 3-D recirculating and turbulent flow in the vessel makes designing and optimizing the reactor usually resorted to pilot plant tests and empirical formulation, even for single phase applications.

A number of investigations have been published on the fluid dynamic properties of solid-liquid systems in stirred vessels for achieving empirical information. Most researches are focused on the distribution of solid particles (Baldi et al., 1981; Barris and Baldi, 1987; MacTaggart et al., 1993; Nasr-El-Din et al., 1987) and the criteria of suspension (Chudacek, 1986; Zwietering, 1958). In recent years, some reported on the flow parameters such as the velocity of two phases of the system with LDV (Nouri and Whitelaw, 1992; Wu et al., 2000).

The empirical approach bears some crucial drawbacks: local information of the system is difficult to obtain, and pilot plant tests are time-consuming and expensive. With the development of computational fluid dynamics (CFD) techniques, numerical method is now more popularly adopted to simulate the flow field in stirred vessels. Most of works reported are on single phase flow in stirred vessels. When a second phase is introduced, the mathematical treatment becomes drastically complex. The main difficulty in simulating the flow field in multi-phase stirred vessels is the accurate representation of the impeller action, the inter-phase interaction and the turbulent quantities. Gosman et al. (1992) calculated the flow in solid-liquid stirred tanks with the Rushton impeller region treated as a 'black box', hence the experimental data had to be imposed on the surface swept by the impeller blades as the boundary conditions. The obvious shortcoming of such approach is that the experimental data in this region is crucially needed for initiating the simulation and it is not applicable to novel operation conditions without experimental measurements. Micale et al. (2000) applied the inner-outer iterative procedure developed by Brucato et al. (1998) to simulate the flow in a solid-liquid stirred vessel. This method does not need experimental data as the impeller region boundary conditions. However, information on the surfaces of the

'inner' and 'outer' domains were averaged over the azimuthal direction thus some important features for the flow in the stirred vessel generated by the periodical rotation of the impeller was ignored. Wang and Mao (2002) improved the inner-outer iterative procedure by combining it with a snapshot approach proposed by Ranade and van den Akker (1994) to keep the unsteady turbulence properties and applied it to simulate the flow in single-phase and gas-liquid stirred vessels. The computational results agreed well with the experimental data.

In this paper, the improved inner-outer iterative procedure is employed to simulate the 3-D solid-liquid flow and the particle distribution in the stirred vessel without requiring experimental data or correlations and to extend the simulation to fairly high solid concentration systems. The present work can be regarded as a necessary step toward the goal of design and scale-up of solid-liquid mixing vessels by numerical simulation.

MATHEMATICAL MODEL

In this work, a 'two-fluid' model proposed by Ishii (1975) is employed to model the solid-liquid flow. In this approach, the continuous phase and the disperse phase are considered to be interpenetrating continua with interaction. The pressure field of the system is assumed to be same for two phases. With above considerations, the governing equations for phase k are

$$\frac{\partial}{\partial t}\rho_k\alpha_k+\frac{\partial}{\partial x_j}\left(\rho_k\alpha_k u_{ki}+\rho_k\overline{\alpha_k' u_{ki}'}\right)=0 \tag{1}$$

$$\rho_k\left(\frac{\partial}{\partial t}(\alpha_k u_{ki})+\frac{\partial}{\partial x_j}\left(\alpha_k u_{ki}u_{kj}\right)\right)= -\alpha_k\frac{\partial P}{\partial x_i}+\rho_k\alpha_k g_i+F_{ki}+\frac{\partial}{\partial x_j}\left(\alpha_k\overline{\tau_{kij}}\right) -\rho_k\frac{\partial}{\partial x_j}\left(\alpha_k\overline{u_{kj}'u_{ki}'}+u_{ki}\overline{u_{kj}'\alpha_k'}+u_{kj}\overline{u_{ki}'\alpha_k'}+\overline{u_{ki}'u_{kj}'\alpha_k'}\right) \tag{2}$$

$$\sum\alpha_k=1.0 \tag{3}$$

where k denotes the phases, d for the dispersed phase and c the continuous. For the closure of momentum equations, the turbulent terms should be related to the known or calculable quantities either via algebraic relations or via differential equations. In the present work, the single phase $k-\varepsilon$ turbulent model is adopted as a basic framework for the simulation for two-phase turbulent flow. The triple and higher order correlations are omitted. The fluctuation of pressure is neglected as well as the viscous shear terms compared with the turbulent shear terms. With the assumption of gradient transport, the velocity correlation, namely Reynolds stresses, are modelled following the practice of single-phase flows as

$$\overline{u_{ki}'u_{kj}'}=-\nu_{kt}\left(\frac{\partial u_{ki}}{\partial x_j}+\frac{\partial u_{kj}}{\partial x_i}\right)+\frac{2}{3}k\delta_{ij} \tag{4}$$

and the correlation between fluctuating velocity and phase fraction gives

$$\overline{u_{ki}'\alpha_k'}=-\frac{\nu_{kt}}{\sigma_t}\frac{\partial\alpha_k}{\partial x_i} \tag{5}$$

where σ_t is the turbulent Schmidt number for the phase dispersion and it is set to unity in this work.

In this way, the final closed momentum equation reads

$$\rho_k\left(\frac{\partial}{\partial t}(\alpha_k u_{ki})+\frac{\partial}{\partial x_j}\left(\alpha_k u_{ki}u_{kj}\right)\right)=-\alpha_k\frac{\partial P}{\partial x_i}+\rho_k\alpha_k g_i+F_{ki} +\frac{\partial}{\partial x_j}\left(\alpha_k\mu_{ke}\left(\frac{\partial u_{ki}}{\partial x_j}+\frac{\partial u_{kj}}{\partial x_i}\right)\right)+\frac{\partial}{\partial x_j}\left(\frac{\mu_{kt}}{\sigma_t}\left(u_{ki}\frac{\partial\alpha_k}{\partial x_j}+u_{kj}\frac{\partial\alpha_k}{\partial x_i}\right)\right) \tag{6}$$

The inter-phase drag force is modelled as

$$F_{ki}=-3\alpha_c\alpha_d C_D\left|\mathbf{U}_d-\mathbf{U}_c\right|\left(u_{di}-u_{ci}\right)/4d_d \tag{7}$$

where C_D is the non-dimensional drag coefficient depended on the particle Reynolds number as

$$C_D=\begin{cases}\dfrac{24}{\mathrm{Re}_d}\left(1+0.15\,\mathrm{Re}_d^{0.687}\right) & \mathrm{Re}_d<1000\\ 0.44 & \mathrm{Re}_d\geq 1000\end{cases} \tag{8}$$

When a non-inertial reference frame is used, the centrifugal force $\mathbf{F}_{r,k}=\alpha_k\rho_k(\boldsymbol{\omega}\times\mathbf{r})\times\boldsymbol{\omega}$ and the Coriolis force $\mathbf{F}_{c,k}=2\alpha_k\rho_k\boldsymbol{\omega}\times\mathbf{u}_k$ will arise.

To close the equations, it still needs some knowledge of the turbulent viscosity, which relates to the turbulent kinetic energy k and the rate of energy dissipation ε. In solid-liquid stirred tanks, the turbulence can mainly be attributed to velocity fluctuation of the liquid phase because the concentration of solid phase is quite low in most part of the tank. The solid phase can affect the turbulence of the system through inter-phase force. The k and ε transport equations of liquid phase can be written in general format as follows:

$$\frac{\partial}{\partial t}(\rho_c\alpha_c\phi)+\frac{\partial}{\partial x_i}(\rho_c\alpha_c u_{ci}\phi)=\frac{\partial}{\partial x_i}\left(\alpha_c\frac{\mu_{ct}}{\sigma_\phi}\frac{\partial\phi}{\partial x_i}\right)+S_\phi \tag{9}$$

where ϕ can be either k or ε and σ_ϕ is the model parameter describing turbulent dispersion of ϕ. The corresponding source terms for k and ε can be written as

$$S_k=\alpha_c\left[(G+G_e)-\rho_c\varepsilon\right] \tag{10}$$

$$S_\varepsilon=\alpha_c\frac{\varepsilon}{k}\left[C_1(G+G_e)-C_2\rho_c\varepsilon\right] \tag{11}$$

The model parameter C_1 is corrected due to the strongly swirling flow in the impeller region:

$$C_1=1.44+\frac{0.8R_f\rho_c\varepsilon}{(G+G_e)} \tag{12}$$

$$R_f=\begin{cases}\dfrac{1}{\varepsilon}\left[\overline{u_r'u_\theta'}\,r\dfrac{\partial}{\partial r}\left(\dfrac{u_\theta}{r}\right)\right] & C-1.5w<z<C+1.5w\\ 0 & z<C-1.5w,\ z>C+1.5w\end{cases} \tag{13}$$

The values of other model parameters are take as proposed in single phase: C_μ=0.09, C_2=1.92, σ_k=1.0, σ_ε=1.3. The turbulent generation term G is given by

$$G=-\rho_c\overline{u_{ci}'u_{cj}'}\frac{\partial u_{ci}}{\partial x_j} \tag{14}$$

G_e is an extra term in the source of the turbulent kinetic energy due to the dispersed phase of particles. Based on analysis of Kataoka et al. (1992), G_e is mainly dependent on the drag force $\boldsymbol{F}$ between two phases which can be modelled as

$$G_e=C_b\left|\boldsymbol{F}\right|\left(\sum\left(u_{ci}-u_{di}\right)^2\right)^{\frac{1}{2}} \tag{15}$$

where C_b is an empirical constant. In the present work, the value is set to 0.03. The turbulent viscosity of continuous phase μ_{ct} is expressed as extended from single phase practice

$$\mu_{ct}=C_\mu\rho_c k^2/\varepsilon \tag{16}$$

and the turbulent viscosity of the dispersed phase μ_{dt} is expressed in terms of the counterpart of the continuous phase via the following formulation:

$$\mu_{dt} = K\mu_{ct} \tag{17}$$

with

$$K = \frac{\rho_d \overline{u'_{di}u'_{di}}}{\rho_c \overline{u'_{ci}u'_{ci}}} \tag{18}$$

Gosman et al. (1992) proposed a correlation of $u_d^{'}$ to $u_c^{'}$ derived from a Lagrangian analysis of particle response to eddies which are much longer than its diameter:

$$u_{di}^{'} = u_{ci}^{'}\left(1 - \exp\left(-\frac{t_l}{t_p}\right)\right) \tag{19}$$

with $t_l = 0.41k/\varepsilon$ being the mean eddy lifetime and t_p, the particle response time, obtained by the Langrangian integration of the equation of motion of a swarm of particles moving through a fluid eddy of given velocity distribution with the expression

$$t_p = \frac{4\rho_d d_d}{3\rho_c C_D \alpha_d |\mathbf{U}_d - \mathbf{U}_c|} \tag{20}$$

Flow in stirred tanks is unsteady for the interaction of rotating impeller blades with stationary baffles. However, the flow pattern will become cyclically repeated once it has fully developed. A snapshot of this flow can describe the flow within the impeller blades at that particular instant. Ranade and van den Akker (1994) suggested that the time derivative terms in governing equations can be ignored without much error in most region of the tank except for the impeller swept volume. In present work, the flow field in the impeller swept volume will be simulated in a non-inertial reference frame rotating with the impeller. Therefore, the time dependent terms will disappear. For other region in the tank, the time derivative terms in the equations can be omitted following Ranade and van den Akker's (1994) analysis. In this way, the resulted model formulation of the mass and momentum conservation equations for phase k in the general form in cylindrical coordinate system reads

$$\begin{aligned}&\frac{1}{r}\frac{\partial}{\partial r}\left(\rho_k r\alpha_k u_{kr}\phi\right) + \frac{1}{r}\frac{\partial}{\partial \theta}\left(\rho_k \alpha_k u_{k\theta}\phi\right) + \frac{\partial}{\partial z}\left(\rho_k \alpha_k u_{kz}\phi\right)\\ &= \frac{1}{r}\frac{\partial}{\partial r}\left(\alpha_k \Gamma_{\varphi eff} r\frac{\partial \phi}{\partial r}\right) + \frac{1}{r}\frac{\partial}{\partial \theta}\left(\frac{\alpha_k \Gamma_{\varphi eff}}{r}\frac{\partial \phi}{\partial \theta}\right)\\ &+ \frac{\partial}{\partial z}\left(\alpha_k \Gamma_{\varphi eff}\frac{\partial \phi}{\partial z}\right) + S_\varphi\end{aligned} \tag{21}$$

NUMERICAL METHODOLOGY

The whole flow field in solid-liquid stirred vessels was simulated at a particular instant. The computational domain was a half of vertical section of the tank due to the symmetry of flow. A modified 'Inner-Outer' iterative procedure (Wang and Mao, 2002) was employed to treat the impeller. In this approach, the whole computational domain is subdivided into two partly overlapping zones, as shown in Fig 1: an 'inner' domain containing the impeller and an 'outer' one, including the wall baffles. The computational procedure includes the following steps:

1. First, the flow in the 'inner' domain was simulated in a reference frame rotating with the impeller, with arbitrary boundary conditions imposed on the surface Σ 2. Centrifugal and Coriolis forces have to be included since the reference frame is non-inertial. Thus a first trial flow field is computed in the whole impeller region including the distribution of flow parameters on the boundary surface Σ 1.
2. The obtained distribution on the boundary surface Σ 1 is used as boundary conditions for simulating the flow in the 'outer' domain carried out in an inertial reference frame. In the present case, the flow parameters on surface Σ 1 were not averaged over azimuthal direction. As a result, information on the whole computational domain is available including the flow parameters on the boundary surface Σ 2.
3. Parameters on the surface Σ 2 are used as boundary conditions for a second 'inner' simulation and so on, until a satisfactory numerical convergence is achieved. Since the reference frames in the 'inner' and 'outer' domain are different, values of the flow parameters have to be converted when exchanging between two domains.

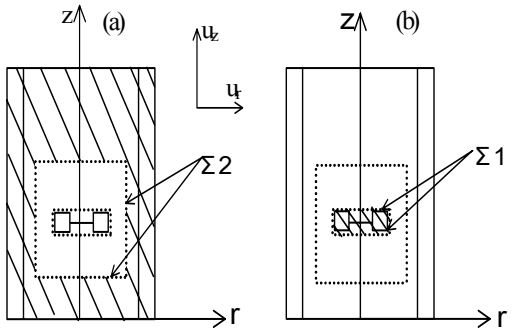

Figure 1: Computational domains for inner-outer procedure (a) inner domain and (b) outer domain, shaded region exclued from the computation

The computational domain is depicted in Fig 2, which consisting of 36, 36 and 90 nodes in the radial, azimuthal and axial directions respectively. The grids selected in the present work is reasonable for the test calculations indicate the difference between the results on grid 36×36 ×90 and on grid 36×36×75 is very small and it is much denser than the 20×15×27 grids used by Gosman et al. (1992) and the 21×64×45 grids used by Altway et al. (2001).

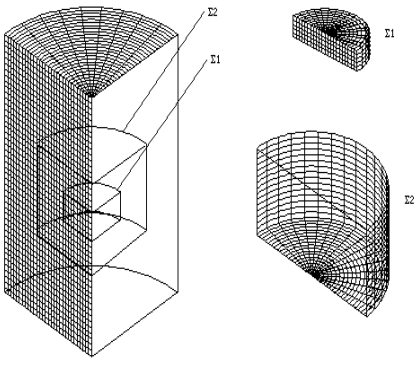

Figure 2: The computational grids of 'inner' and 'outer' domains. Both grids coincide with each other on the surfaces Σ1 and Σ2

The governing equations are solved by a control volume method. Discretization of the partial differential equations

is obtained by integration over each control volume using a staggered arrangement of variables with a 'power-law' scheme (Patankar, 1980). The SIMPLE algorithm was adopted to solve for velocity and pressure coupling. The resulted equations connect the value of a variable ϕ at each cell-centered node to its nearest neighbours by algebraic relations of the form

$$a_{\mathrm{p}}\phi_{\mathrm{p}} = \sum_{\mathrm{nb}} a_{\mathrm{nb}}\phi_{\mathrm{nb}} + b \tag{22}$$

For two phases flow, there are two continuity equations should be satisfied at the same time. Therefore, an algorithm has to be set up to obtain the pressure and the volume fraction of each phase. In this work, it is assumed that two phases share the same pressure and the pressure-correction should fit each phase. The two continuity equations are combined together to obtain the pressure-correction formula as the following

$$\left[\left(a_{\mathrm{p}}\right)_{\mathrm{c}} + \left(a_{\mathrm{p}}\right)_{\mathrm{d}}\right] p'_{\mathrm{P}} = \sum_{\mathrm{nb}} \left[\left(a_{\mathrm{nb}}\right)_{\mathrm{c}} + \left(a_{\mathrm{nb}}\right)_{\mathrm{d}}\right] p'_{\mathrm{nb}} + f_{\mathrm{c}} + f_{\mathrm{d}} + D_{\mathrm{c}} + D_{\mathrm{d}} \tag{23}$$

where p' denotes the pressure correction, f_{k} is the turbulent diffusive mass transport, and D_{k} is the imbalance of continuity equations. The volume fraction of the continuous phase is obtained by solving its continuity equation and the volume fraction of the dispersed phase can then be obtained from Eq. (3). The sets of discretized equations for each variable are solved iteratively by means of an ADI technique. The non-linearities in the phase momentum and turbulence equations are handled by standard under-relaxation techniques.

RESULTS

This work simulated the flow field in the solid-liquid stirred vessel for a case where experimental data were available (Nouri and Whitelaw, 1992). The geometric configuration is T=H=0.294m, C=D=T/3. The dispersed phase is glass particles with ρ_{d}=2950 kg/m^3, d_{d}=232.5 μm, the solid concentration is 0.02% and N=300rpm.

The predicted mean velocity fields of two phases are presented as velocity vector plots shown in Fig. 3. It can be observed that the mean velocity field of solid phase is similar to that of liquid, which means that the solid particles trace the liquid closely. In the present work, an important but seldom reported feature is demonstrated. In the velocity vector of solid phase, a small recirculation loop appears near the tank axis below the impeller due to the accumulation of the solid particles in this region. This phenomenon has been reported by Nagata (1975) and Chudacek (1985).

The distribution of solid particles in the stirred vessel was not reported by Nouir and van den Akker (1992) but was predicted by Gosman et al. (1992) who presented a contour map of the normalized solid concentration. In this work, the similar calculation is carried out and the result agrees well with Gosman et al's (1992) result. From Fig.4 it is also observed that the maximum solid concentration occurs on the centre of the tank bottom, the level gradually decreases from the bottom to the free liquid surface. The solid concentration contour shows a small circular region with low concentration below the impeller plane, which is confirmed by the presence of circulation flow depicted in the velocity vector plot. In the region above the impeller plane, there is also a circulation flow but without a region with low solid concentration.

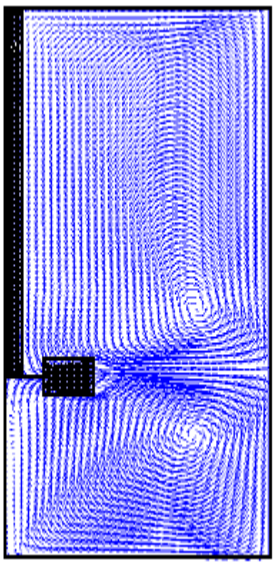

liquid phase

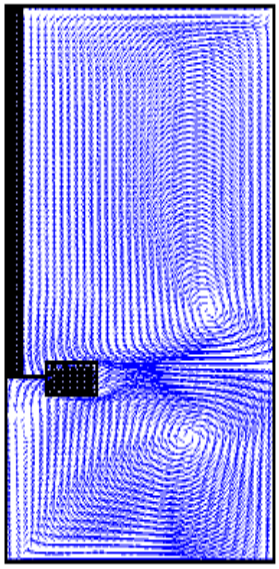

solid phase

Figure 3: Velocity vector plots

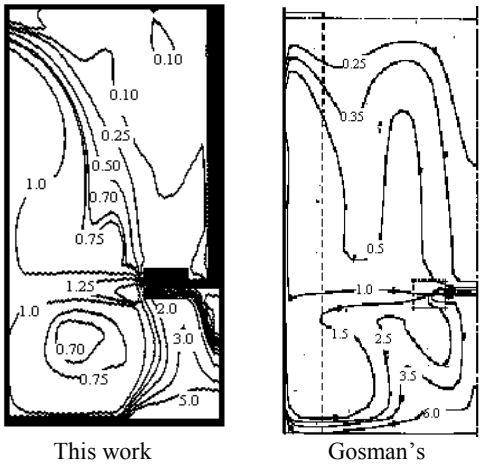

This work Gosman's

Figure 4: The normalized solid concentration contour

Comparisons of predicted mean velocity of solid phase with the experiment data from Nouri and Whitelaw (1992) are shown in Fig.5. The mean velocity of liquid phase is also mapped. The mean radial velocities of the solid and liquid phase are much similar and agree well with the experiment results especially in the location away from the blade. In the region close to the impeller, there is some discrepancies which can mainly attributed to the standard isotropic $k-\varepsilon$ turbulence model used in simulation while the turbulent flow in the impeller stream region is strongly anisotropic.

For the axial profiles of the mean velocities of solid and liquid phase, the simulation results are all well predicted below and above the impeller plane. It is readily seen that the axial velocities of the solid phase are always below those of the liquid due to the fact that the solid particles are heavier than the liquid.

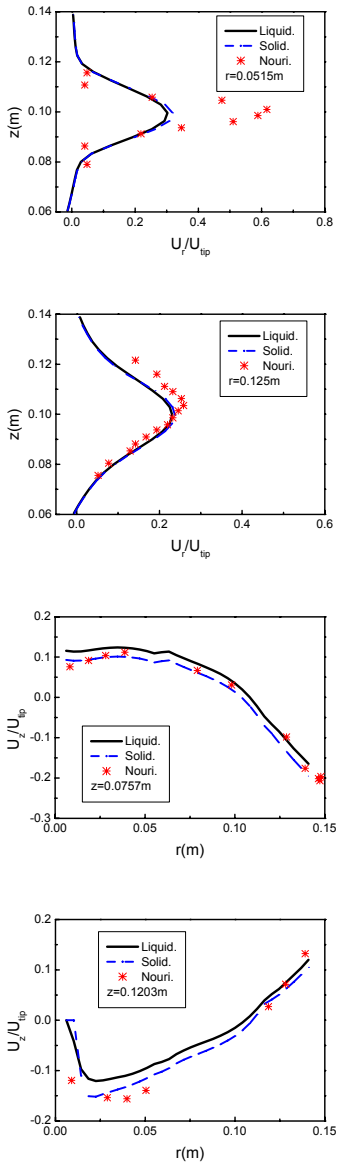

Figure 5: Comparisons of mean velocity

The solid concentration profiles measured by Yamazaki et al. (1986) is also simulated in this work with the operation condition T=H=0.30m， D=C=T/3， N=800rpm， ρ_d= 2360 kg/m^3， d_d=87 μm and the averaged solid concentrations are $\alpha_{d,av}$=5% and $\alpha_{d,av}$=20% respectively. The comparisons of simulation results with the experimental data are shown in Fig.6. It is observed that the simulation coincides well with the experiment even for high solid concentration. The distribution of the solid phase is much homogeneous for high rotating speed. The peak of concentration is shown on the impeller plane which was also observed by Barresi and Baldi (1987) and verified by Altway et al. (2001).

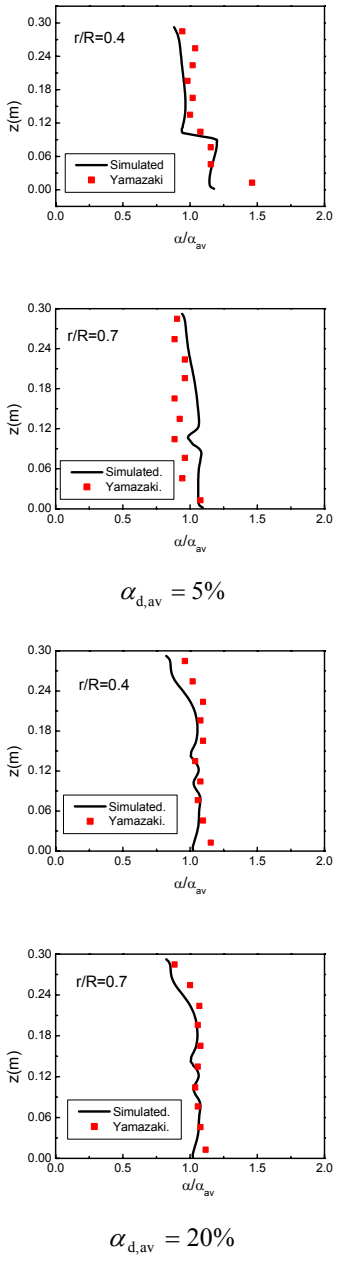

Figure 6: Comparison of solid concentration distribution

CONCLUSION

Flow field and solid concentration distribution in a solid-liquid stirred vessel with a standard Rushton disc impeller are simulated using an improved inner-outer procedure. The simulation results agree well with the experimental data. The recirculation loop at the center of the tank below the impeller where solid particles accumulate is

demonstrated numerically for the first time. The predicted results for the solid concentration distribution in the tank shows the procedure used in the present work can be applied to the system with high solid concentration up to 20%. Moreover, this procedure can be extended to other systems for it does not need experimental data as boundary conditions, thus having the potential of being used to scale-up and design of related process equipment.

ACKNOWLEDGMENTS

Authors acknowledge the financial support of the National Natural Science Foundation of China (Nos. 20006015, 20236050).

REFERENCES

ALTWAY, A., SETYAWAN, H., MARGONO, and WINARDI, S., (2001), "Effect of particle size on the simulation of three-dimensional solid dispersion in stirred tank", *Trans. IchemE*, **79**, 1011-1016.

BALDI, G., CONTI, R., and GIANETTO, A., (1981), "Concentration profile for solids suspended in a continuous agitated reactor", *AIChE J.*, **27**, 1017-1020.

BARRESI, A., and BALDI, G., (1987), "Solid dispersion in an agitated vessel", *Chem. Eng. Sci.*, **42**, 2949-2956

BRUCATO, A., CIOFALO, M., GRISAFI, F., and MICALE, G., (1998), "Numerical prediction of flow fields in baffled stirred vessels: a comparison of alternative modeling approaches", *Chem. Eng. Sci.*, **53**, 3653-3684.

CHUDACEK, M.W., (1985), "Solids suspension behavior in profiled bottom and flat bottom mixing tanks", *Chem. Eng. Sci.*, **40**, 385-392

CHUDACEK, M.W., (1986), "Relationship between solids suspension criteria, mechanism of suspension, tank geometry, and scale-up parameters in stirred tank", *Ind. Eng. Chem. Fundam.*, **25**, 391-401

GOSMAN, A.D., and IDERIAH, F.J.K., (1976), "Teach T: A general computer program for modeling of two-dimensional, turbulent, recirculating flows", The lecture in Imperial College

GOSMAN, A. D., ISSA, R. I., LEKAKOU, C., LOONEY, M. K., and POLITIS, S., (1992), "Multidimensional modeling of turbulent two-phase flows in stirred vessels", *AIChE J.*, **38**, 1946-1956.

ISHII, M., (1975), *Thermo-fluid Dynamic Theory of Two Phase Flows,* Paris, Eyrolles

KATAOKA, I., BESNARD, D.C., and SERIZAWA, A., (1992), "Basic equation of turbulence and modeling of interfacial transfer terms in gas-liquid two-phase flow", *Chem. Eng. Commun.,* **118**, 221-231

LAUNDER, B.E., and SPALDING, D.B., (1974), "The numerical computation of turbulent flows", *Comput. Meth. Appl. Mech. Eng.,* **3**, 269-285

LJUNGQVIST, M., and RASMUSON, A., (2001), "Numerical simulation of the two-phase flow in an axially stirred vessel". *Trans. IchemE.*, **79**, 533-546.

MACTAGGART, R.S., NASR-El-DIN, H.A., and MASLIYAH, J.H., (1993), "Sample withdrawal from a slurry mixing tank", *Chem. Eng. Sci.*, **48**, 921-931

MICALE, G., MONTANTE, G., GRISAFI, F., BRUCATO, A., and Godfrey, J., (2000), "CFD simulation of particle distribution in stirred vessels", *Trans. IchemE.*, **78**, 435-443.

MONTANTE, G., MICALE, G., MAGELLI, F., and BRUCATO, A., (2001), "Experiments and CFD predictions of solid particle distribution in a vessel agitated with pitched blade turbines", *Trans. IchemE.*, **79**, 1005-1010.

NASR-EL-DIN, H.A., SHOOK, C.A., and COLWELL, J., (1987), "A conductivity probe for measuring local concentration in slurry systems", *Int. J. Multiphase Flow.,* **13**, 365-378

NOURI, J.M., and WHITELAW, J.H., (1992), "Particle velocity characteristics of dilute to moderately dense suspension flows in stirred reactors", *Int. J. Multiphase Flow.*, **18**, 21-33

NAGATA, S., (1975), *Mixing: Principles and Applications,* Halsted Press.

PATANKAR, S.V., (1980), *Numerical Heat Transfer and Fluid Flow,* New York, McGraw-Hill.

RANADE, V.V., and VAN DEN AKKER, H.E.A., (1994), "A computational snapshot of gas-liquid flow in baffled stirred reactors", *Chem. Eng. Sci*, **49**, 5175-5192.

WANG, W.J, and MAOD, Z.S., (2002), "Numerical simulation of gas-liquid flow in a stirred tank with a Rushton impeller", *Chinese J. Chem. Eng.,* **10**, 285-295.

WU, J., ZHU, Y., BANDOPADHAYAY, P.C., PULLUM, L., and SHEPHERD, I.C., (2000), "Solids suspension with axial—flow impellers", *AIChE J.*, **46**, 647-650.

YAMAZAKI, H., TOJO, K., and MIYANAMI, K., (1986), "Concentration profiles of solids suspended in a stirred tank", *Adv. Powder. Tech.*, **48**, 205-216

ZWIETERING, T.N., (1958), "Suspending of solid particles in liquid by agitators", *Chem. Eng. Sci*, **8**, 244-253.